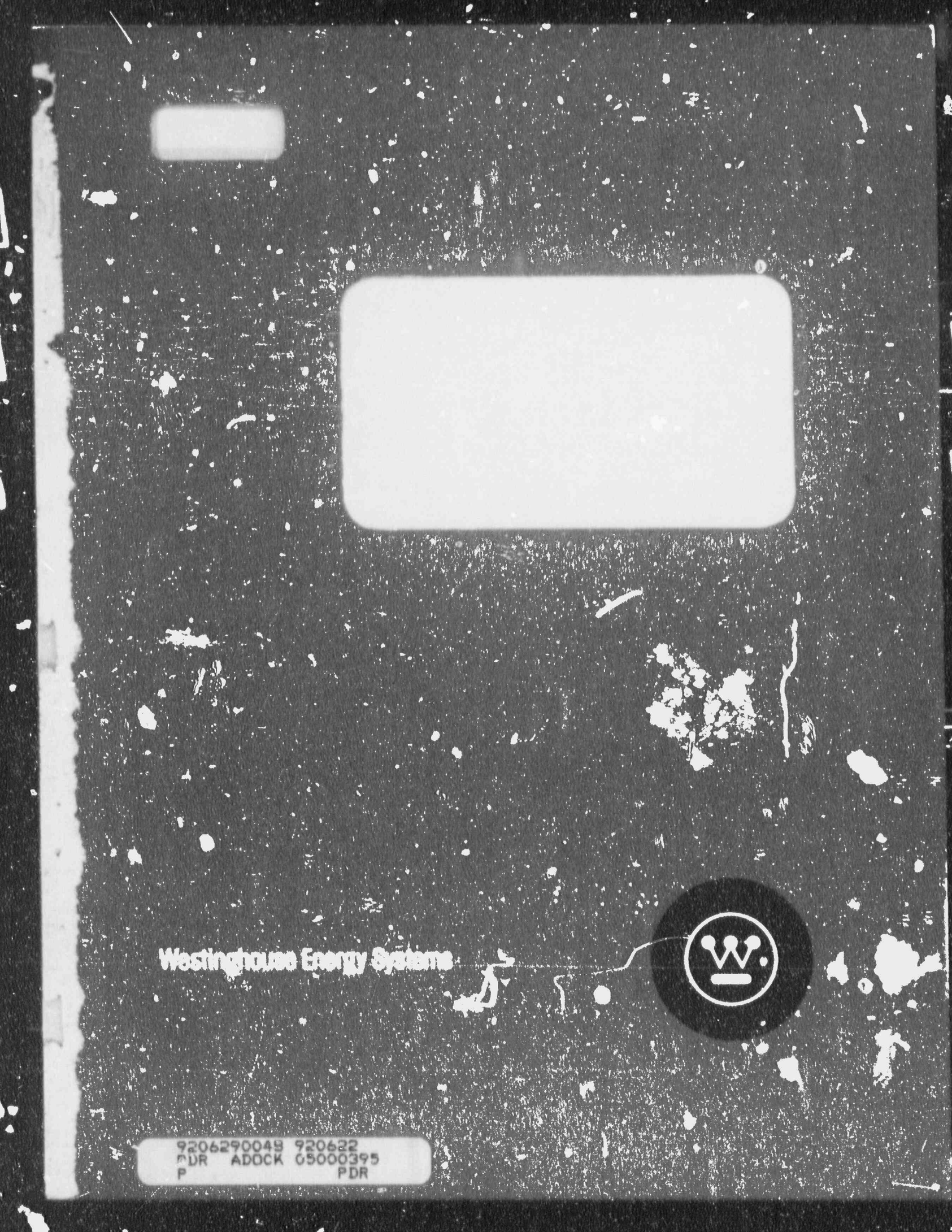

WCAP-13207

TECHNICAL JUSTIFICATION FOR ELIMINATING LARGE PRIMARY LOOP PIPE RUPTURE AS THE STRUCTURAL DESIGN BASIS FOR THE VIRGIL C. SUMMER NUCLEAR POWER PLANT

APRIL 1992

J. C. Schmertz
S. A. Swamy
Y. S. Lee

VERIFIED: _____
F. O. Witt

APPROVED: _____ 4/10/92
D. C. Adamonis, Acting Manager
Structural Mechanics Technology

Work Performed Under Shop Order VSPP-950

WESTINGHOUSE ELECTRIC CORPORATION
Nuclear and Advanced Technology Division
P. O. Box 2728
Pittsburgh, Pennsylvania 15230-2728

FOREWORD

This document contains Westinghouse Electric Corporation proprietary information and data which has been identified by brackets. Coding associated with the brackets sets forth the basis on which the information is considered proprietary. These codes are listed with their meanings in WCAP-7211.

The proprietary information and data contained in this report were obtained at considerable Westinghouse expense and its release could seriously affect our competitive position. This information is to be withheld from public disclosure in accordance with the Rules of Practice 10 CFR 2.790 and the information presented herein be safeguarded in accordance with 10 CFR 2.903. Withholding of this information does not adversely affect the public interest.

This information has been provided for your internal use only and should not be released to persons or organizations outside the Directorate of Regulation and the ACRS without the express written approval of Westinghouse Electric Corporation. Should it become necessary to release this information to such persons as part of the review procedure, please contact Westinghouse Electric Corporation, which will make the necessary arrangements required to protect the Corporation's proprietary interests.

TABLE OF CONTENTS

TABLE OF CONTENTS

TABLE OF CONTENTS

LIST OF TABLES

LIST OF TABLES (Cont'd)

LIST OF FIGURES

LIST OF FIGURES (Cont'd)

EXECUTIVE SUMMARY

The existing structural design basis for the reactor coolant system of the Virgil C. Summer nuclear reactor power plant requires that the dynamic effects of pipe breaks be evaluated and that protective measures for such breaks be incorporated into the design. However, within the last decade, such breaks have been shown to be highly unlikely and should not be included, in general, in the structural design basis of Westinghouse type pressurized water reactors, for example. To eliminate primary loop pipe breaks from the design basis, it must be demonstrated to the satisfaction of the U.S. Nuclear Regulatory Commission that a leak-before-break situation exists. This report provides such a demonstration for the Virgil C. Summer nuclear power plant.

In this report it is shown that the primary loops are highly resistant to stress corrosion cracking and high and low cycle fatigue. Water hammer is mitigated by system design and operating procedures.

The primary loops were extensively examined. The as-built geometries for the pipe and elbows and loadings were obtained. The materials were evaluated using the Certified Materials Test Reports. Mechanical properties were determined at operating temperatures. Since the piping systems are fabricated from cast stainless steel, fracture toughnesses considering thermal aging were determined for each heat of material.

Based on loading, pipe geometry and fracture toughness considerations, enveloping critical locations were determined at which leak-before-break crack stability evaluations were made. Through-wall flaw sizes were found which would leak at a rate of ten times the leakage detection system capability of the plant. Large margins for such flaw sizes were shown against flaw instability. Finally, fatigue crack growth was shown not to be an issue for the primary loops.

It is concluded that dynamic effects of reactor coolant system primary loop pipe breaks need not be considered in the structural design basis of the Virgil C. Summer nuclear power plant.

SECTION 1.0
INTRODUCTION

1.1 Purpose

This report applies to the Virgil C. Summer Nuclear Power Plant Reactor Coolant System (RCS) primary loop piping. It is intended to demonstrate that for the specific parameters of the Virgil C. Summer plant, RCS primary loop pipe breaks need not be considered in the structural design basis. The approach taken has been accepted by the Nuclear Regulatory Commission (NRC) (reference 1-1).

1.2 Scope

The existing structural design basis for the RCS primary loop requires that dynamic effects of pipe breaks be evaluated. Specifically, as part of the Loss of Coolant Accident (LOCA) design basis for the Virgil C. Summer plant the following breaks are postulated in the RCS primary loop piping: the six terminal ends in the cold, hot, and crossover legs; a split in the steam generator inlet elbow, and the loop closure weld in the crossover leg. However, Westinghouse has demonstrated on a generic basis that RCS primary loop pipe breaks are highly unlikely and should not be included in the structural design basis of Westinghouse plants (see reference 1-2). In order to demonstrate this applicability of the generic evaluations to the Virgil C. Summer plant, Westinghouse has performed a fracture mechanics evaluation, a determination of leak rates from a through-wall crack, a fatigue crack growth evaluation, and an assessment of margins against crack instability consistent with the leak-before-break (LBB) methodology. Through this successful application of the LBB methodology, the above eight break locations in the RCS primary loop piping are eliminated from the Virgil C. Summer plant's structural design basis.

1.3 Objectives

In order to validate the elimination of RCS primary loop pipe breaks for the Virgil C. Summer plant, the following objectives must be achieved:

a. Demonstrate that margin exists between the critical crack size and a postulated crack which yields a detectable leak rate.

b. Demonstrate that there is sufficient margin between the leakage through a postulated crack and the leak detection capability of the Virgil C. Summer plant.

c. Demonstrate margin on applied load.

d. Demonstrate that fatigue crack growth is negligible.

1.4 Background Information

Westinghouse has performed considerable testing and analysis to demonstrate that RCS primary loop pipe breaks can be eliminated from the structural design basis of all Westinghouse plants. The concept of eliminating pipe breaks in the RCS primary loop was first presented to the NRC in 1978 in WCAP-9283 (reference 1-3). That topical report employed a deterministic fracture mechanics evaluation and a probabilistic analysis to support the elimination of RCS primary loop pipe breaks. That approach was then used as a means of addressing Generic Issue A-2 and Asymmetric LOCA Loads.

Westinghouse performed additional testing and analysis to justify the elimination of RCS primary loop pipe breaks. This material was provided to the NRC along with Letter Report NS-EPR-2519 (reference 1-4).

The NRC funded research through Lawrence Livermore National Laboratory (LLNL) to address this same issue using a probabilistic approach. As part of the LLNL research effort, Westinghouse performed extensive evaluations of specific plant loads, material properties, transients, and system geometries to demonstrate that the analysis and testing previously performed by Westinghouse and the research performed by LLNL applied to all Westinghouse plants

(references 1-5 and 1-6). The results from the LLNL study were released at a March 28, 1983, ACRS Subcommittee meeting. These studies which are applicable to all Westinghouse plants east of the Rocky Mountains determined the mean probability of a direct LOCA (RCS primary loop pipe break) to be 4.4×10^{-12} per reactor year and the mean probability of an indirect LOCA to be 10^{-7} per reactor year. Thus, the results previously obtained by Westinghouse (reference 1-3) were confirmed by an independent NRC research study.

Based on the studies by Westinghouse, LLNL, the ACRS, and the AIF, the NRC completed a safety review of the Westinghouse reports submitted to address asymmetric blowdown loads that result from a number of discrete break locations on the PWR primary systems. The NRC Staff evaluation (reference 1-1) concludes that an acceptable technical basis has been provided so that asymmetric blowdown loads need not be considered for those plants that can demonstrate the applicability of the modeling and conclusions contained in the Westinghouse response or can provide an equivalent fracture mechanics demonstration of the primary coolant loop integrity. In a more formal recognition of LBB methodology applicability for PWRs, the NRC appropriately modified 10 CFR 50, General Design Criterion 4, "Requirements for Protection Against Dynamic Effects for Postulated Pipe Rupture" (reference 1-7).

This report provides a fracture mechanics demonstration of primary loop integrity for the Virgil C. Summer plant consistent with the NRC position for exemption from consideration of dynamic effects.

Several computer codes are used in the evaluations. The main-frame computer programs are under Configuration Control which has requirements conforming to Standard Review Plan 3.9.1. The fracture mechanics calculations are independently verified (benchmarked).

1.5 References

1-1 USNRC Generic Letter 84-04, Subject: "Safety Evaluation of Westinghouse Topical Reports Dealing with Elimination of Postulated Pipe Breaks in PWR Primary Main Loops," February 1, 1984.

1-2 Letter from Westinghouse (E. P. Rahe) to NRC (R. H. Vollmer), NS-EPR-2768, dated May 11, 1983.

1-3 WCAP-9283, "The Integrity of Primary Piping Systems of Westinghouse Nuclear Power Plants During Postulated Seismic Events," March, 1978.

1-4 Letter Report NS-EPR-2519, Westinghouse (E. P. Rahe) to NRC (D. G. Eisenhut), Westinghouse Proprietary Class 2, November 10, 1981.

1-5 Letter from Westinghouse (E. P. Rahe) to NRC (W. V. Johnston) dated April 25, 1983.

1-6 Letter from Westinghouse (E. P. Rahe) to NRC (W. V. Johnston) dated July 25, 1983.

1-7 Nuclear Regulatory Commission, 10 CFR 50, Modification of General Design Criteria 4 Requirements for Protection Against Dynamic Effects of Postulated Pipe Ruptures, Final Rule, Federal Register/Vol. 52, No. 207/Tuesday, October 27, 1987/Rules and Regulations, pp. 41288-41295.

SECTION 2.0

OPERATION AND STABILITY OF THE REACTOR COOLANT SYSTEM

2.1 Stress Corrosion Cracking

The Westinghouse reactor coolant system primary loops have an operating history that demonstrates the inherent operating stability characteristics of the design. This includes a low susceptibility to cracking failure from the effects of corrosion (e.g., intergranular stress corrosion cracking). This operating history totals over 450 reactor-years, including five plants each having over 17 years of operation and 15 other plants each with over 12 years of operation.

In 1978, the United States Nuclear Regulatory Commission (USNRC) formed the second Pipe Crack Study Group. (The first Pipe Crack Study Group established in 1975 addressed cracking in boiling water reactors only.) One of the objectives of the second Pipe Crack Study Group (PCSG) was to include a review of the potential for stress corrosion cracking in Pressurized Water Reactors (PWR's). The results of the study performed by the PCSG were presented in NUREG-0531 (reference 2-1) entitled "Investigation and Evaluation of Stress Corrosion Cracking in Piping of Light Water Reactor Plants." In that report the PCSG stated:

> "The PCSG has determined that the potential for stress-corrosion cracking in PWR primary system piping is extremely low because the ingredients that produce IGSCC are not all present. The use of hydrazine additives and a hydrogen overpressure limit the oxygen in the coolant to very low levels. Other impurities that might cause stress-corrosion cracking, such as halides or caustic, are also rigidly controlled. Only for brief periods during reactor shutdown when the coolant is exposed to the air and during the subsequent startup are conditions even marginally capable of producing stress-corrosion cracking in the primary systems of PWRs. Operating experience in PWRs supports this determination. To date, no stress corrosion cracking has been reported in the primary piping or safe ends of any PWR."

During 1979, several instances of cracking in PWR feedwater piping led to the establishment of the third PCSG. The investigations of the PCSG reported in NUREG-0691 (reference 2-2) further confirmed that no occurrences of IGSCC have been reported for PWR primary coolant systems.

As stated above, for the Westinghouse plants there is no history of cracking failure in the reactor coolant system loop. The discussion below further qualifies the PCSG's findings.

For stress corrosion cracking (SCC) to occur in piping, the following three conditions must exist simultaneously: high tensile stresses, susceptible material, and a corrosive environment. Since some residual stresses and some degree of material susceptibility exist in any stainless steel piping, the potential for stress corrosion is minimized by properly selecting a material immune to SCC as well as preventing the occurrence of a corrosive environment. The material specifications consider compatibility with the system's operating environment (both internal and external) as well as other material in the system, applicable ASME Code rules, fracture toughness, welding, fabrication, and processing.

The elements of a water environment known to increase the susceptibility of austenitic stainless steel to stress corrosion are: oxygen, fluorides, chlorides, hydroxides, hydrogen peroxide, and reduced forms of sulfur (e.g., sulfides, sulfites, and thionates). Strict pipe cleaning standards prior to operation and careful control of water chemistry during plant operation are used to prevent the occurrence of a corrosive environment. Prior to being put into service, the piping is cleaned internally and externally. During flushes and preoperational testing, water chemistry is controlled in accordance with written specifications. Requirements on chlorides, fluorides, conductivity, and Ph are included in the acceptance criteria for the piping.

During plant operation, the reactor coolant water chemistry is monitored and maintained within very specific limits. Contaminant concentrations are kept below the thresholds known to be conducive to stress corrosion cracking with the major water chemistry control standards being included in the plant operating procedures as a condition for plant operation. For example, during normal power operation, oxygen concentration in the RCS is expected to be in

the ppb range by controlling charging flow chemistry and maintaining hydrogen in the reactor coolant at specified concentrations. Halogen concentrations are also stringently controlled by maintaining concentrations of chlorides and fluorides within the specified limits. Thus during plant operation, the likelihood of stress corrosion cracking is minimized.

2.2 Water Hammer

Overall, there is a low potential for water hammer in the RCS since it is designed and operated to preclude the voiding condition in normally filled lines. The reactor coolant system, including piping and primary components, is designed for normal, upset, emergency, and faulted condition transients. The design requirements are conservative relative to both the number of transients and their severity. Relief valve actuation and the associated hydraulic transients following valve opening are considered in the system design. Other valve and pump actuations are relatively slow transients with no significant effect on the system dynamic loads. To ensure dynamic system stability, reactor coolant parameters are stringently controlled. Temperature during normal operation is maintained within a narrow range by control rod position; pressure is controlled by pressurizer heaters and pressurizer spray also within a narrow range for steady-state conditions. The flow characteristics of the system remain constant during a fuel cycle because the only governing parameters, namely system resistance and the reactor coolant pump characteristics, are controlled in the design process. Additionally, Westinghouse has instrumented typical reactor coolant systems to verify the flow and vibration characteristics of the system. Preoperational testing and operating experience have verified the Westinghouse approach. The operating transients of the RCS primary piping are such that no significant water hammer can occur.

2.3 Low Cycle and High Cycle Fatigue

Low cycle fatigue considerations are accounted for in the design of the piping system through the fatigue usage factor evaluation to show compliance with the rules of Section III of the ASME Code. A further evaluation of the low cycle fatigue loadings was carried out as part of this study in the form of a fatigue crack growth analysis, as discussed in section 8.0.

High cycle fatigue loads in the system would result primarily from pump vibrations. These are minimized by restrictions placed on shaft vibrations during hot functional testing and operation. During operation, an alarm signals the exceedence of the vibration limits. Field measurements have been made on a number of plants during hot functional testing, including plants similar to the Virgil C. Summer. Stresses in the elbow below the reactor coolant pump resulting from system vibration have been found to be very small, between 2 and 3 ksi at the highest. These stresses are well below the fatigue endurance limit for the material and would also result in an applied stress intensity factor below the threshold for fatigue crack growth.

2.4 References

2-1 Investigation and Evaluation of Stress-Corrosion Cracking in Piping of Light Water Reactor Plants, NUREG-0531, U.S. Nuclear Regulatory Commission, February 1979.

2-2 Investigation and Evaluation of Cracking Incidents in Piping in Pressurized Water Reactors, NUREG-0691, U.S. Nuclear Regulatory Commission, September 1980.

SECTION 3.0
PIPE GEOMETRY AND LOADING

3.1 Introduction to Methodology

The general approach is discussed first. As an example a segment of the primary coolant hot leg pipe is shown in figure 3-1. The as-built outside diameter and minimum wall thickness of the pipe are 33.90 in. and 2.205 in., respectively, as seen in the figure. Normal stresses at the weld locations result from the load combination procedure discussed in section 3.3 while faulted loads are developed as outlined in section 3.4. The components for normal loads are pressure, dead weight and thermal expansion. An additional component, Safe Shutdown Earthquake (SSE), is considered for faulted loads. As seen later the highest stressed location in the entire loop is at the reactor vessel outlet nozzle to pipe weld. This highest stressed location is a load critical location and is one of the locations at which, as an enveloping location, leak-before-break is to be established. Essentially a circumferential flaw is postulated to exist at this location thus the normal loads and faulted loads must be available to assess leakage and stability, respectively. The loads (developed below) at this location are also given in Figure 3-1.

Since the elbows are cast stainless steel, thermal aging must be considered (see section 4.0). Thermal aging results in lower fracture toughness criteria; thus, other locations than the load critical locations must be examined taking into consideration both fracture toughness and stress. The enveloping locations so determined are called toughness critical locations. The single most critical location is apparent only after the full analysis is completed. Once loads (this section) and fracture toughnesses (section 4.0) are available, the load critical and toughness critical locations are determined (see section 5.0). At these locations, leak rate evaluations (see section 6.0) and fracture mechanics evaluations (see section 7.0) are performed per the guidance of Reference 3-1. Fatigue crack growth (see section 8.0) and stability margins are also evaluated (see section 9.0).

The locations for evaluation are those shown in figure 3-2.

3.2 Calculation of Loads and Stresses

The stresses due to axial loads and bending moments are calculated by the following equation:

(3-1)

$$\sigma = \frac{F}{A} + \frac{M}{Z}$$

where,

σ	=	stress
F	=	axial load
M	=	bending moment
A	=	pipe cross-sectional area
Z	=	section modulus

The bending moments for the desired loading combinations are calculated by the following equation:

(3-2)

$$M = \sqrt{M_Y^2 + M_Z^2}$$

where,

M	=	bending moment for required loading
M_Y	=	Y component of bending moment
M_Z	=	Z component of bending moment

The axial load and bending moments for leak rate predictions and crack stability analyses are computed by the methods to be explained in sections 3.3 and 3.4.

3.3 Loads for Leak Rate Evaluation

The normal operating loads for leak rate predictions are calculated by the following equations:

$$F = F_{DW} + F_{TH} + F_P \quad (3\text{-}3)$$

$$M_Y = (M_Y)_{DW} + (M_Y)_{TH} + (M_Y)_P \quad (3\text{-}4)$$

$$M_Z = (M_Z)_{DW} + (M_Z)_{TH} + (M_Z)_P \quad (3\text{-}5)$$

The subscripts of the above equations represent the following loading cases:

DW = deadweight
TH = normal thermal expansion
P = load due to internal pressure

This method of combining loads is often referred as the algebraic sum method.

The loads based on this method of combination are provided in Table 3-1 at all the locations identified in Figure 3-2. The as-built dimensions are also given.

3.4 Load Combination for Crack Stability Analyses

In accordance with Standard Review Plan 3.6.3 the absolute sum of loading components can be applied which results in higher magnitude of combined loads. If crack stability is demonstrated using these loads, the LBB margin on loads can be reduced from √2 to 1.0. The absolute summation of loads results in the following equations:

$$F = |F_{DW}| + |F_{TH}| + |F_P| + |F_{SSEINERTIA}| + |F_{SSEAM}| \quad (3\text{-}6)$$

$$M_Y = |(M_Y)_{DW}| + |(M_Y)_{TH}| + |(M_Y)_P| + |(M_Y)_{SSEINERTIA}| + |(M_Y)_{SSEAM}| \quad (3\text{-}7)$$

$$M_Z = |(M_Z)_{DW}| + |(M_Z)_{TH}| + |(M_Z)_P| + |(M_Z)_{SSEINERTIA}| + \quad (3\text{-}8)$$

$$|(M_Z)_{SSEAM}|$$

where subscripts SSE, INERTIA and AM mean safe shutdown earthquake, inertia and anchor motion, respectively.

The loads so determined are used in the fracture mechanics evaluations (section 7.0) to demonstrate the LBB margins at the locations established to be the governing locations. These loads at all the locations of interest (see Figure 3-2) are given in Table 3-2.

3.5 References

3-1 USNRC Standard Review Plan 3.6.3, Leak-Before-Break Evaluation Procedures, NUREG-0800.

TABLE 3-1

DIMENSIONS, NORMAL LOADS AND NORMAL STRESSES FOR

VIRGIL C. SUMMER

Location[a]	Outside Diameter (in.)	Minimum Thickness (in.)	Axial Load[b] (kips)	Bending Moment (in-kips)	Stress (ksi)
1	33.90	2.205	1476	22052	20.21
2	33.90	2.205	1500	3600	9.03
3	36.23	2.349	1590	9677	11.22
4	36.23	2.349	1588	5675	9.71
5	36.20	2.340	1567	5952	9.30
6	36.20	2.340	1562	6484	9.55
7	36.20	2.340	1687	718	7.14
8	36.20	2.340	1687	3341	8.46
9	36.20	2.340	1840	11138	13.02
10	32.20	2.070	1392	4131	10.08
11	32.20	2.070	1392	3987	9.98
12	32.20	2.070	1391	4449	10.31

a See figure 3-2

b Includes pressure

TABLE 3-2

FAULTED LOADS AND STRESSES FOR

VIRGIL C. SUMMER

Location[a,b]	Axial Load[c] (Kips)	Bending Moment (in-Kips)	Total Stress (ksi)
1	1857	23996	23.14
2	1843	11101	15.19
3	2049	17721	17.10
4	1887	17281	16.23
5	1893	18455	16.93
6	1888	11554	13. 2
7	1842	7084	10.98
8	1828	10212	12.50
9	1905	16457	15.96
10	1883	17789	22.43
11	1906	10952	17.62
12	1824	11769	17.79

a See Figure 3-2
b See table 3-1 for dimensions
c Includes pressure

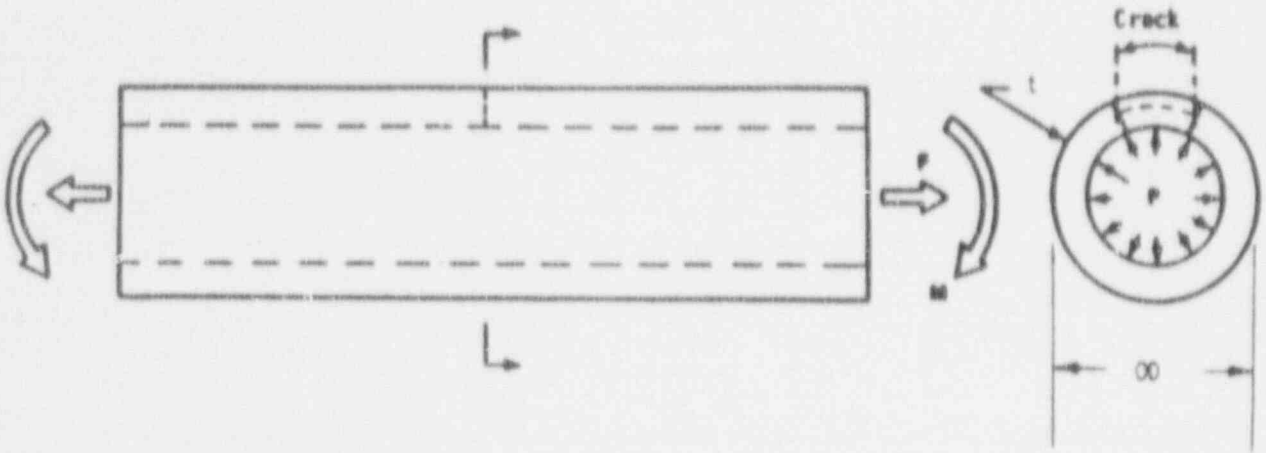

OD = 33.90 in

t = 2.205 in

Normal Loads		Faulted Loads	
force[a]:	1476 kips	force[a]:	1857 kips
bending moment:	22052 in-kips	bending moment:	23996 in-kips

[a]Includes the force due to a pressure of 2250 psi

Figure 3-1

Hot Leg Coolant Pipe

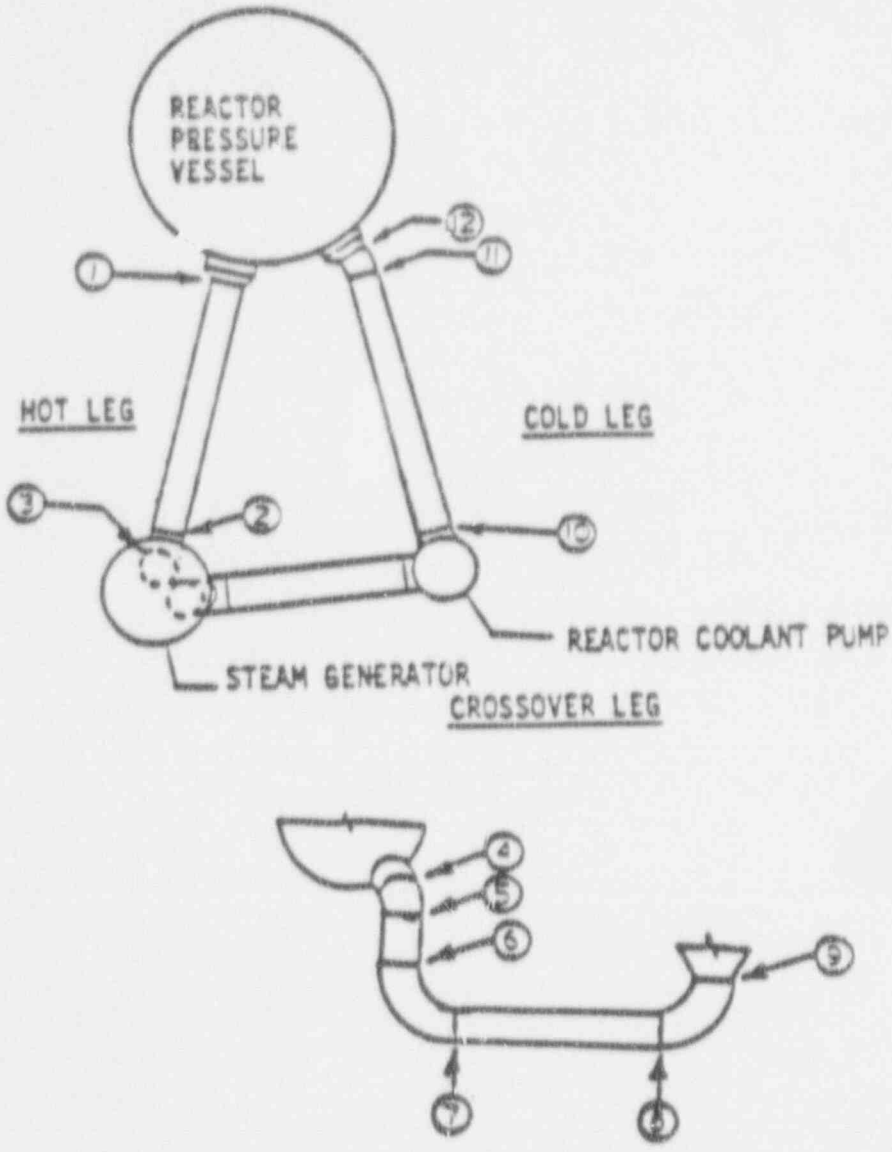

HOT LEG

Temperature 619°F, Pressure: 2250 psi

CROSSOVER LEG

Temperature 556°F, Pressure: 2250 psi

COLD LEG

Temperature 556°F, Pressure: 2250 psi

Figure 3-2

Schematic Diagram of Virgil C. Summer Primary Loop Showing Weld Locations

SECTION 4.0
MATERIAL CHARACTERIZATION

4.1 Primary Loop Pipe and Fittings Materials

The primary loop pipe materials are SA376 TP304N, and the elbow fittings are SA351 CF8A.

4.2 Tensile Properties

The Certified Materials Test Reports (CMTRs) for Virgil C. Summer were used to establish the tensile properties for the leak-before-break analyses. The CMTRs include tensile properties at room temperature for each of the heats of material. These properties are given for Virgil C. Summer in Table 4-1. The average properties are given and the lower bound properties are identified.

For the SA351 CF8A material, the properties at 619°F and 556°F were established from the tensile properties at room temperature given in Table 4-1 by utilizing Table 4-2. Plant D of Table 4-2 provides typical tensile properties at room temperature and at 650°F for SA351 CF8A. Typical tensile properties for SA351 CF8A at 619°F and 556°F were obtained by interpolating between the room temperature and the 650°F tensile properties given in Table 4-2. Ratios of the tensile properties at 619°F and 556°F to the corresponding tensile properties at room temperature for the typical material were then applied to the room temperature values given in Table 4-1 to obtain the plant specific properties for SA351 CF8A at 619°F and 556°F.

For the SA376 TP304N material, the properties at 619°F and 556°F were established from the tensile properties at room temperature given in Table 4-1 by utilizing Section III of the 1989 ASME Boiler and Pressure Vessel Code. Code tensile properties at 619°F and 556°F were obtained by interpolating between the room temperature and the 650°F tensile properties. Ratios of the tensile properties at 619°F and 556°F to the corresponding tensile properties at room temperature were then applied to the room temperature values given in Table 4-1 to obtain the plant specific properties for SA376 TP304N at 619°F and 556°F.

The average and lower bound yield strengths and ultimate strengths are given in Table 4-3. The ASME Code moduli of elasticity are also given, and Poisson's ratio was taken as 0.3.

For leak-before-break fracture evaluations of the toughness critical locations the true stress-true strain curves for SA351 CF8A at 619°F and 556°F must be available. These curves were obtained using the Nuclear Systems Materials Handbook (reference 4-1). The lower bound true stress-true strain curves are given in Figures 4-1 and 4-2.

4.3 Fracture Toughness Properties

The pre-service fracture toughnesses of both forged and cast stainless steels of interest here have in terms of J been found to be very high at 600°F. Typical results for a cast material are observed to be over 2500 in-lbs/in^2. Forged materials are even higher. However, cast stainless steels are subject to thermal aging during service. This thermal aging causes an elevation in the yield strength of the material and a degradation of the fracture toughness, the degree of degradation being somewhat proportional to the level of ferrite in the material.

To determine the effects of thermal aging on piping integrity, a detailed study was carried out in reference 4-2. In that report, fracture toughness results were presented for a material [

]^{a,c,e} The effects of the aging process on the end-of-service life fracture toughness are further discussed in Appendix B.

End-of-service life toughnesses for the heats are established using the alternate toughness criteria methodology of reference 4-5 (Appendix B). By

that methodology a heat of material is said to be as good as [ ]^{a,c,e} if it can be demonstrated that its end-of-service fracture toughnesses equal or exceed those of [

]^{a,c,e} . As taken from Appendix B, the fracture toughness for all three loops at each location (see figure 3-2) is as good as or better than the [ ]^{a,c,e} toughness.

Available data on aged stainless steel welds (references 4-2 and 4-3) indicate that J_{Ic} values for the worst case welds are of the same order as the aged material. However, the slope of the J-R curve is steeper, and higher J-values have been obtained from fracture tests (in excess of 3000 in-lb/in^2). The applied value of the J-integral for a flaw in the weld regions will be lower than that in the base metal because the yield stress for the weld materials is much higher at temperature[a]. Therefore, weld regions are less limiting than the cast material.

Forged stainless steel piping such as SA376 TP304N does not degrade due to thermal aging. Thus fracture toughness values well in excess of that established for the cast material and welds exist for this material throughout service life and are not limiting.

4.4 References

4-1 Nuclear Systems Materials Handbook, Part I - Structural Materials, Group 1 - High Alloy Steels, Section 2, ERDA Report TID 26666, November, 1975.

4-2 WCAP 10456, "The Effects of Thermal Aging on the Structural Integrity of Cast Stainless Steel Piping for W NSSS," W Proprietary Class 2, November 1983.

---

[a] In the report all the applied J values were conservatively determined by using base metal strength properties.

4-3 Slama, G., Petrequin, P., Masson, S.H., and Mager, T R., "Effect of Aging on Mechanical Properties of Austenitic Stainless Steel Casting and Welds", presented at Smirt 7 Post Conference Seminar 6 - Assuring Structural Integrity of Steel Reactor Pressure Boundary Components, August 29/30, 1983, Monterey, CA.

4-4 Appendix II of Letter from Dominic C. DiIanni, NRC to D. M. Musolf, Northern States Power Company, Docket Nos. 50-282 and 50-306, December 22, 1986.

4-5 Witt, F.J., Kim, C.C., "Toughness Criteria for Thermally Aged Cast Stainless Steel," WCAP-10931, Revision 1, Westinghouse Electric Corporation, July 1986, (Westinghouse Proprietary Class 2).

TABLE 4-1
MEASURED ROOM TEMPERATURE TENSILE PROPERTIES
FOR VIRGIL C. SUMMER PRIMARY
LOOP PIPING AND FITTINGS

Component	Loop	Heat No.	Material	Yield Strength (ksi)	Ultimate Strength (ksi)
			PIPE	Room Temp.	Room Temp.
Hot Leg	A	L1359/14462	SA376 TP304N	48.0 49.7	87.7 92.7
Hot Leg	B	L1359/14463	SA376 TP304N	47.2 49.7	88.4 92.4
Hot Leg	C	L1359/14464	SA376 TP304N	45.9 49.7	88.7 91.7
Crossover Leg	A	K3723/15903X	SA376 TP304N	46.5 48.2	89.7 91.4
Crossover Leg	B	K3723/15903Y	SA376 TP304N	46.5 48.2	89.7 91.4
Crossover Leg	B	K3723/15692X	SA376 TP304N	45.0 48.0	87.4 91.4
Crossover Leg	C	K3723/15903Z	SA376 TP304N	46.5 48.2	89.7 91.4
Crossover Leg	C	K3723/15692Y	SA376 TP304N	45.0 48.0	87.4 91.4
Cold Leg	A	L1336/14461	SA376 TP304N	40.9 45.9	82.1 88.6
Cold Leg	B	K3723/16098	SA376 TP304N	43.7 45.9	86.4 89.9
Cold Leg	C	L1551/17989	SA376 TP304N	48.5 43.7	92.2 86.1
				1028.9	
Average				46.8	

Room Temp. Minimum Yield Strength: 40.9 ksi
Room Temp. Minimum Ultimate Strength: 82.1 ksi
Room Temp. Average Yield Strength: 46.8 ksi

TABLE 4-1 (continued)
MEASURED ROOM TEMPERATURE TENSILE PROPERTIES
VIRGIL C. SUMMER PRIMARY
LOOP PIPING AND FITTINGS

Component	Loop	Heat No.	Material	Yield Strength (ksi)	Ultimate Strength (ksi)
			FITTINGS	Room Temp.	Room Temp.
Hot Leg	A	79420-1	SA351 CF8A	38.1	81.5
Hot Leg	B	79420-2	SA351 CF8A	38.1	81.5
Hot Leg	C	80019-2	SA351 CF8A	31.2	77.7
Crossover Leg	A	90946-1	SA351 CF8A	38.7	86.7
Crossover Leg	A	[illegible]723/15692W	SA351 CF8A	45.0 (46.5) 48.0	87.4 (89.4) 91.4
Crossover Leg	A	89916-1	SA351 CF8A	44.3	86.9
Crossover Leg	B	92293-1	SA351 CF8A	38.2	82.2
Crossover Leg	B	89253-1	SA351 CF8A	42.5	85.7
Crossover Leg	C	91068-1	SA351 CF8A	37.3	82.5
Crossover Leg	C	93212-1	SA351 CF8A	37.9	83.7
Crossover Leg	A or B or C[a]	84013-1	SA351 CF8A	39.3	83.5
Crossover Leg	A or B or C[a]	84227-1	SA351 CF8A	40.5	82.5
Crossover Leg	A or B or C[a]	82695-2	SA351 CF8A	37.2	82.4
Cold Leg	A	67487-1	SA351 CF8A	43.6	86.5
Cold Leg	B	65692-2	SA351 CF8A	39.3	83.6
Cold Leg	C	73359-4	SA351 CF8A	37.0	85.9
				169.2	
Average				39.3	

Room Temp. Minimum Yield Strength: 31.2 ksi
Room Temp. Minimum Ultimate Strength: 77.7 ksi
Room Temp. Average Yield Strength: 39.3 ksi

a) Could not be identified as to the applicable loop

TABLE 4-2

TYPICAL TENSILE PROPERTIES OF SA376 TP316, SA351 CF8A AND WELDS OF SUCH MATERIAL FOR THE PRIMARY LOOP

Plant	Material	Test Temperature (°F)	Average Tensile Properties	
			Yield (psi)	Ultimate (psi)

a,c,e

[redacted]

TABLE 4-3
MECHANICAL PROPERTIES FOR VIRGIL C. SUMMER
MATERIALS AT OPERATING TEMPERATURES

Material	Temperature (°F)	Average Yield Strength (psi)	Lower Bound Yield Stress (psi)	Lower Bound Ultimate Strength (psi)
[				] a,c,e

Modulus of Elasticity

$E = 25.21 \times 10^6$ psi. at 619°F
$E = 25.52 \times 10^6$ psi. at 556°F

Poisson's ratio: 0.3

Figure 4-1

Representative Lower Bound True Stress - True Strain Curve for
SA351 CF8A at 619°F

Figure 4-2

Representative Lower Bound True Stress - True Strain Curve for
SA351 CF8A at 556°F

Figure 4-3

J Vs. Δa at Different Temperatures for Aged Material
[Heat L]^{a,c,e} (7500 Hours at 400°C)

SECTION 5.0
CRITICAL LOCATIONS AND EVALUATION CRITERIA

5.1 Critical Locations

The leak-before-break (LBB) evaluation margins are to be demonstrated for the limiting locations (governing locations). Candidate locations are designated load critical locations or toughness critical locations as discussed in Section 3.0. Such locations are established considering the loads (section 3.0) and the material properties established in section 4.0. These locations are defined below for Virgil C. Summer. Table 3-2 as well as Figure 3-2 are used for this evaluation.

Load Critical Locations

The highest stressed location for the SA376 TP304N straight pipes is location 1. For the weaker SA351 CF8A elbows the highest stressed location at 619°F (the hot leg) temperature is location 3, and the highest stressed location at 556°F (the cold leg) temperature is location 12. These are the three load critical locations. (Note that although the stress is lower at location 3 than at location 12, the material is weaker because it is at the higher temperature). Thus locations 3 and 12 both are considered as load critical locations.

Toughness Critical Locations

Low toughness locations are at the ends of every elbow. All the elbows exceed the toughness of [ ].[a,c,e] Hence, for all the elbows the toughness allowables are J_{ic} [ ]^{a,c,e} The highest stressed elbow is at location 12 where the temperature is 556°F. Where the temperature is 619°F, and hence the yield strength and tensile strength are lower, the highest stressed elbow is at location 3. Thus locations 3 and 12 are also the toughness critical locations.

5.2 Fracture Criteria

As will be discussed later, fracture mechanics analyses are made based on loads and postulated flaw sizes related to leakage. The stability criteria against which the calculated J (i.e. J_{app}) and tearing modulus (T_{app}) are compared are:

(1) If $J_{app} < J_{Ic}$, then the crack is stable;

(2) If $J_{app} \geq J_{Ic}$, then, if $T_{app} < T_{mat}$

and $J_{app} < J_{max}$, the crack is stable.

These criteria apply to the toughness critical locations. For load critical locations, the limit load method discussed in Section 7.0 is used.

SECTION 6.0
LEAK RATE PREDICTIONS

6.1 Introduction

The purpose of this section is to discuss the method which is used to predict the flow through postulated through-wall cracks and present the leak rate calculation results for through-wall circumferential cracks.

6.2 General Considerations

The flow of hot pressurized water through an opening to a lower back pressure causes flashing which can result in choking. For long channels where the ratio of the channel length, L, to hydraulic diameter, D_H, (L/D_H) is greater than [ ]^{a,c,e}, both [

]^{a,c,e}.

6.3 Calculation Method

The basic method used in the leak rate calculations is the method developed by [

]

The flow rate through a crack was calculated in the following manner. Figure 6-1 from Reference 6-1 was used to estimate the critical pressure, Pc, for the primary loop enthalpy condition and an assumed flow. Once Pc was found for a given mass flow, the [ ]^{a,c,e} was found from Figure 6-2 taken from Reference 6-1. For all cases considered, since [ ]^{a,c,e} Therefore, this method will yield the two-phase pressure drop due to momentum effects as illustrated in Figure 6-3.

Now using the assumed flow rate, G, the frictional pressure drop can be calculated using

$$\Delta P_f = [\quad]^{a,c,e} \tag{6-1}$$

where the friction factor f is determined using the [ ]^{a,c,e} The crack relative roughness, ε, was obtained from fatigue crack data on stainless steel samples. The relative roughness value used in these calculations was [ ]^{a,c,e}

The frictional pressure drop using equation 6-1 is then calculated for the assumed flow and added to the [ ]^{a,c,e} to obtain the total pressure drop from the primary system to the atmosphere. That is, for the primary loop

$$\text{Absolute Pressure} - 14.7 = [\quad]^{a,c,e} \tag{6-2}$$

for a given assumed flow G. If the right-hand side of equation 6-2 does not agree with the pressure difference between the primary loop and the atmosphere, then the procedure is repeated until equation 6-2 is satisfied to within an acceptable tolerance and this results in the flow value through the crack.

6.4 Leak Rate Calculations

Leak rate calculations were made as a function of crack length at the governing locations previously identified in section 5.1. The normal operating loads of Table 3-1 were applied, in these calculations. The crack opening areas were estimated using the method of Reference 6-2 and the leak rates were calculated using the two-phase flow formulation described above. The average material properties of section 4.0 were used for these calculations.

The flaw sizes to yield a leak rate of 10 gpm were calculated at the governing locations and are given in Table 6-1. The flaw sizes so determined are called leakage flaws.

The Virgil C. Summer plant RCS pressure boundary leak detection system meets the intent of Regulatory Guide 1.45. Thus, to satisfy the margin of 10 on the leak rate, the flaw sizes (leakage flaws) are determined which yield a leak rate of 10 gpm.

6.5 References

6-1 [

]^{a,c,e}.

6-2 Tada, H., "The Effects of Shell Corrections on Stress Intensity Factors and the Crack Opening Area of Circumferential and a Longitudinal Through-Crack in a Pipe," Section II-1, NUREG/CR-3464, September 1983.

TABLE 6-1

FLAW SIZES YIELDING A LEAK RATE OF

10 GPM AT THE GOVERNING LOCATIONS

a,c,e

[ ]

Figure 6-1 Analytical Predictions of Critical Flow Rates of Steam-Water Mixtures

a,c,e

Figure 6-2 [Critical or Choked]^{a,c,e} Pressure Ratio as a Function of L/D

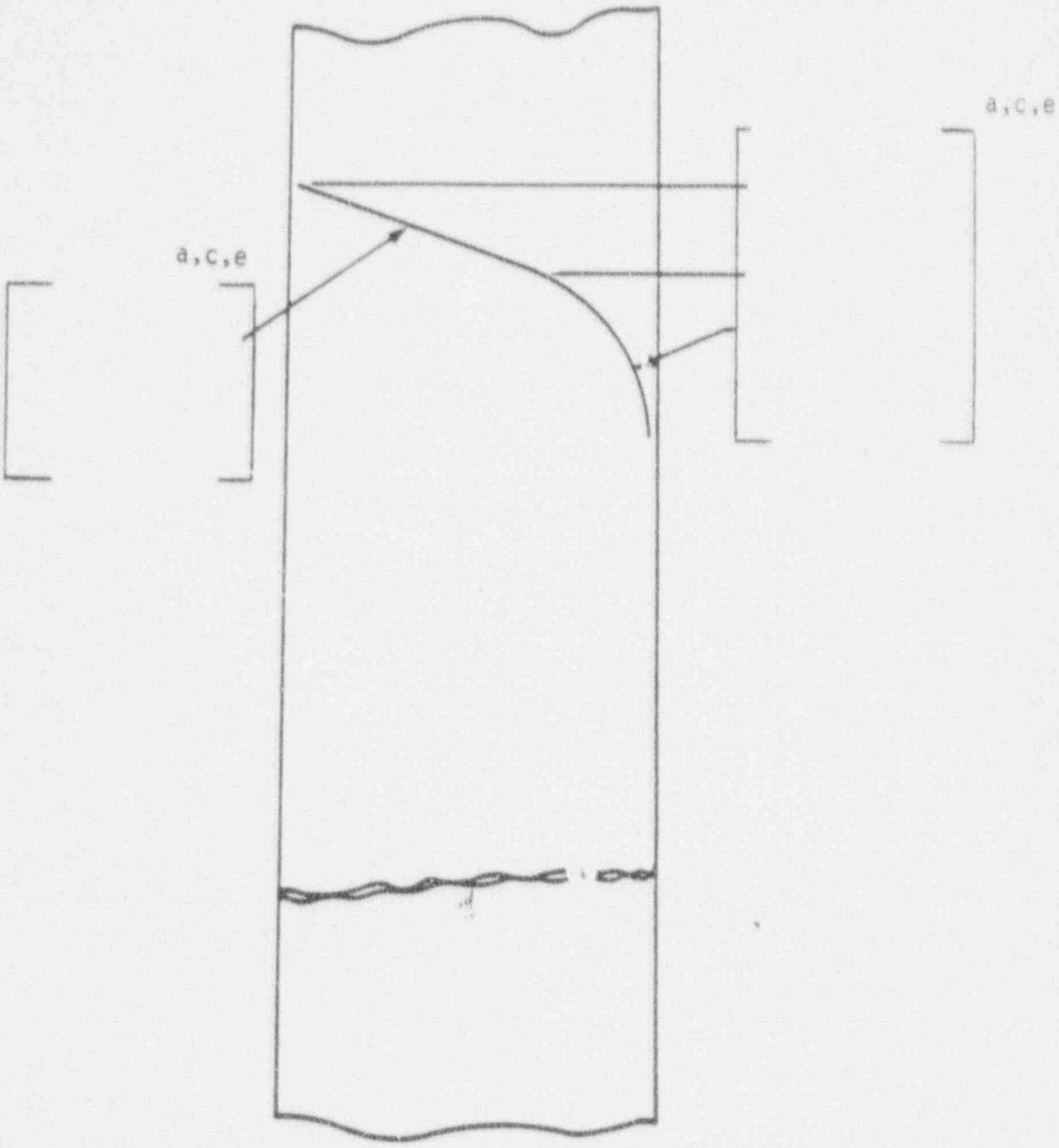

Figure 6-3 Idealized Pressure Drop Profile Through a Postulated Crack

SECTION 7.0
FRACTURE MECHANICS EVALUATION

7.1 Local Failure Mechanism

The local mechanism of failure is primarily dominated by the crack tip behavior in terms of crack-tip blunting, initiation, extension and finally crack instability. The local stability will be assumed if the crack does not initiate at all. It has been accepted that the initiation toughness measured in terms of J_{Ic} from a J-integral resistance curve is a material parameter defining the crack initiation. If, for a given load, the calculated J-integral value is shown to be less than the J_{Ic} of the material, then the crack will not initiate. If the initiation criterion is not met, one can calculate the tearing modulus as defined by the following relation:

$$T_{app} = \frac{dJ}{da} \frac{E}{\sigma_f^2}$$

where:

T_{app}	=	applied tearing modulus
E	=	modulus of elasticity
σ_f	=	$0.5\ (\sigma_y + \sigma_u)$ (flow stress)
a	=	crack length
σ_y, σ_u	=	yield and ultimate strength of the material, respectively

Stability is said to exist when ductile tearing occurs if T_{app} is less than T_{mat}, the experimentally determined tearing modulus. Since a constant T_{mat} is assumed a further restriction is placed in J_{app}. J_{app} must be less than J_{max} where J_{max} is the maximum value of J for which the experimental T is greater than or equal to the T_{mat} used.

As discussed in Section 5.2 the local crack stability will be established by the two-step criteria:

(1) If $J_{app} < J_{Ic}$, then the crack is stable.

(2) If $J_{app} \geq J_{Ic}$, then, if $T_{app} < T_{mat}$

and $J_{app} < J_{max}$, the crack is stable.

7.2 Global Failure Mechanism

Determination of the conditions which lead to failure in stainless steel should be done with plastic fracture methodology because of the large amount of deformation accompanying fracture. One method for predicting the failure of ductile material is the plastic instability method, based on traditional plastic limit load concepts, but accounting for strain hardening and taking into account the presence of a flaw. The flawed pipe is predicted to fail when the remaining net section reaches a stress level at which a plastic hinge is formed. The stress level at which this occurs is termed as the flow stress. The flow stress is generally taken as the average of the yield and ultimate tensile strength of the material at the temperature of interest. This methodology has been shown to be applicable to ductile piping through a large number of experiments and will be used here to predict the critical flaw size in the primary coolant piping. The failure criterion has been obtained by requiring equilibrium of the section containing the flaw (figure 7-1) when loads are applied. The detailed development is provided in appendix A for a through-wall circumferential flaw in a pipe with internal pressure, axial force, and imposed bending moments. The limit moment for such a pipe is given by:

[ ]^{a,c,e}

where:

[

]^{a,c,e}

[

]a,c,e

The analytical model described above accurately accounts for the piping internal pressure as well as imposed axial force as they affect the limit moment. Good agreement was found between the analytical predictions and the experimental results (reference 7-1).

For application of the limit load methodology, the material, including consideration of the configuration, must have a sufficient ductility and ductile tearing resistance to sustain the limit load.

7.3 Results of Crack Stability Evaluation

Stability analyses were performed at the critical locations established in section 5.1. The elastic-plastic fracture mechanics (EPFM) J-integral analyses for through-wall circumferential cracks in a cylinder were performed using the procedure in the EPRI fracture mechanics handbook (reference 7-2).

The lower-bound material properties of section 4.0 were applied (see Table 4-3). The fracture toughness properties established in section 4.3 and the normal plus SSE loads given in Table 3-2 were used for the EPFM calculations. Evaluations were performed at the toughness critical locations identified in section 5.1. The results of the elastic-plastic fracture mechanics J-integral evaluations are given in Table 7-1. The leakage size flaws are presented on the same table.

The load critical locations were also identified in section 5.1. A stability analysis based on limit load was performed for these locations as described in section 7.2. Since the welds at these locations are all SMAW welds, the "Z" factor correction for SMAW welds was applied (Reference 7-3) as follows:

$$Z = 1.15\ [1.0 + 0.013\ (OD-4)]$$

where OD is the outer diameter of the pipe in inches.

The Z-factors were calculated for the load critical locations, using the dimensions given in table 3-1. The Z factors were 1.60, 1.63, and 1.57 for locations 1, 3 and 12 respectively. The applied loads were increased by the Z factors and plots of limit load versus crack length were generated as shown in Figures 7-2, 7-3 and 7-4. Table 7-2 gives the results of the stability analyses based on limit load.

7.4 References

7-1. Kanninen, M. F., et. al., "Mechanical Fracture Predictions for Sensitized Stainless Steel Piping with Circumferential Cracks," EPRI NP-192, September 1976.

7-2. Kumar, V., German, M. D. and Shih, C. P., "An Engineering Approach for Elastic-Plastic Fracture Analysis," EPRI Report NP-1931, Project 1237-1, Electric Power Research Institute, July 1981.

7-3. ASME Code Section XI, Winter 1985 Addendum, Article IWB-3640.

TABLE 7-1

STABILITY RESULTS FOR VIRGIL C. SUMMER
BASED ON ELASTIC-PLASTIC
J-INTEGRAL EVALUATIONS

		Fracture Criteria			Calculated Values	
Location	Flaw Size (in)	J_{Ic} (in-lb/in^2)	T_{mat}	J_{max} (in-lb/in^2)	J_{app} (in-lb/in^2)	T_{app}
[						] a,c,e

TABLE 7-2

STABILITY RESULTS FOR VIRGIL C. SUMMER
BASED ON LIMIT LOAD

Location	Flaw Size (in.)	Leakage Flaw Size (in.)
[		] a,c,e

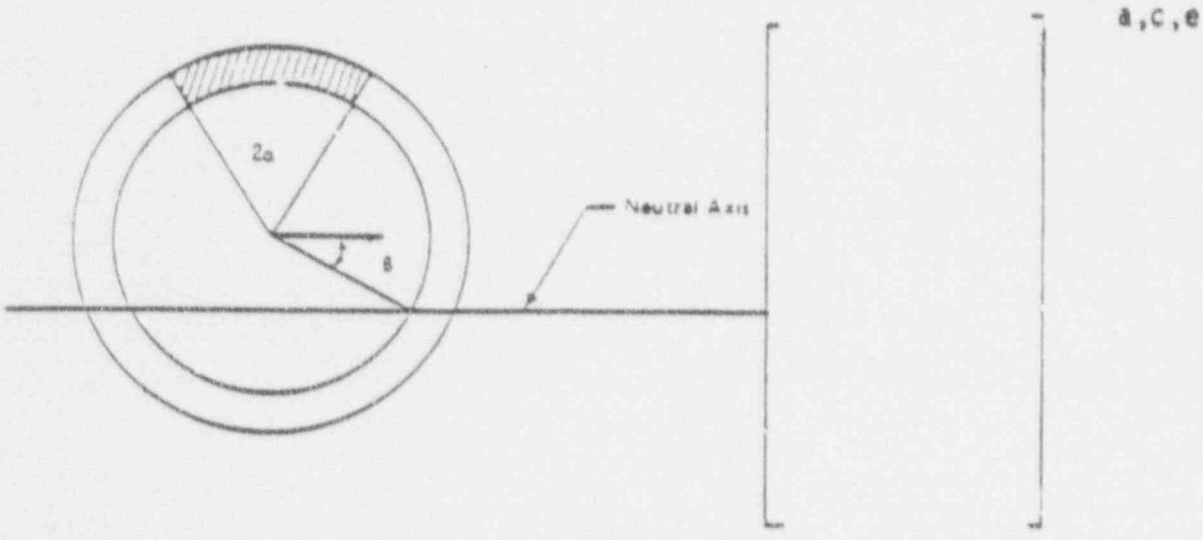

a,c,e

Figure 7-1

[ ]^{a,c,e} Stress Distribution

a,c,e

O_U	= 33.90 in	σ_y	= 23.8 ksi	F_a	= 1857 kips
t	= 2.205 in	σ_u	= 71.5 ksi	M_b	= 23996 in-kips

SA376 TP304N Material With SMAW Weld

Figure 7-2
Critical Flaw Size Prediction - Hot Leg at Location 1

a,c,e

OD	= 36.23 in	σ_y	= 17.9 ksi	F_a	= 2049 kips
t	= 2.349 in	σ_u	= 56.8 ksi	M_b	= 17721 in-kips

SA351 CF3A Material With SMAW Weld

Figure 7-3
Critical Flaw Size Prediction - Hot Leg at Location 3

a,c,e

OD = 32.20 in σ_y = 19.4 ksi F_e = 1824 kips

t = 2.07 in σ_u = 59.2 ksi M_b = 11769 in-kips

SA351 CF8A Material With SMAW Weld

Figure 7-4

Critical Flaw Size Prediction - Cold Leg at Location 12

SECTION 8.0
FATIGUE CRACK GROWTH ANALYSIS

To determine the sensitivity of the primary coolant system to the presence of small cracks, a fatigue crack growth analysis was carried out for the [ ]^{a,c,e} region of a typical system (see Location [ ]^{a,c,e} of Figure 3-2). This region was selected because crack growth calculated here will be typical of that in the entire primary loop. Crack growths calculated at other locations can be expected to show less than 10% variation.

A [ ]^{a,c,e} of a plant typical in geometry and operational characteristics to any Westinghouse PWR System. [ ]^{a,c,e} All normal, upset, and test conditions were considered. A summary of the applied transients is provided in table 8-1. Circumferentially oriented surface flaws were postulated in the region, assuming the flaw was located in three different locations, as shown in Figure 8-1. Specifically, these were:

Cross Section A: [ ]^{a,c,e}
Cross Section B: [ ]^{a,c,e}
Cross Section C: [ ]^{a,c,e}

Fatigue crack growth rate laws were used [ ]^{a,c,e} The law for stainless steel was derived from Reference 8-1, with a very conservative correction for the R ratio, which is the ratio of minimum to maximum stress during a transient. For stainless steel, the fatigue crack growth formula is:

$$\frac{da}{dn} = (5.4 \times 10^{-12}) \; K_{eff}^{4.48} \; inches/cycle$$

where $K_{eff} = K_{max} \; (1-R)^{0.5}$

$R = K_{min}/K_{max}$

[

]^{a,c,e}

[ ]^{a,c,e}

where: [ ]^{a,c,e}

The calculated fatigue crack growth for semi-elliptic surface flaws of circumferential orientation and various depths is summarized in Table 8-2, and shows that th ck growth is very small, [

]^{a,c,}

8.1 References

8-1 Bamford, W. H., "Fatigue Crack Growth of Stainless Steel Piping in a Pressurized Water Reactor Environment," Trans. ASME Journal of Pressure Vessel Technology, Vol. 101, Feb. 1979.

8-2 [

]^{a,c,e}

8-3 [

]^{a,c,e}

TABLE 8-1

SUMMARY OF REACTOR VESSEL TRANSIENTS

NUMBER	TYPICAL TRANSIENT IDENTIFICATION	NUMBER OF CYCLES
	Normal Conditions	
1	Heatup and Cooldown at 100°F/hr (pressurizer cooldown 200°F/hr)	200
2	Load Follow Cycles (Unit loading and unloading at 5% of full power/min)	18300
3	Step load increase and decrease	2000
4	Large step load decrease, with steam dump	200
5	Steady state fluctuations	10^6
	Upset Conditions	
6	Loss of load, without immediate turbine or reactor trip	80
7	Loss of power (blackout with natural circulation in the Reactor Coolant System)	40
8	Loss of Flow (partial loss of flow, one pump only)	80
9	Reactor trip from full power	400
	Test Conditions	
10	Turbine roll test	10
11	Hydrostatic test conditions	
	Primary side	5
	Primary side leak test	50
12	Cold Hydrostatic test	10

TABLE 8-2

TYPICAL FATIGUE CRACK GROWTH AT
[ ]^{a,c,e} (40 YEARS)

	FINAL FLAW (in)		
Initial Flaw (in)	[ ]^{a,c,e}	[ ]^{a,c,e}	[ ]^{a,c,e}
0.292	0.31097	0.30[illegible]	0.30698
0.300	0.31949	0.30[illegible]	0.31626
0.375	0.39940	0.3894[illegible]	0.40763
0.425	0.45271	0.4435	0.47421

Figure 8-1

Typical Cross-Section of [ ]a,c,e

a,c,e

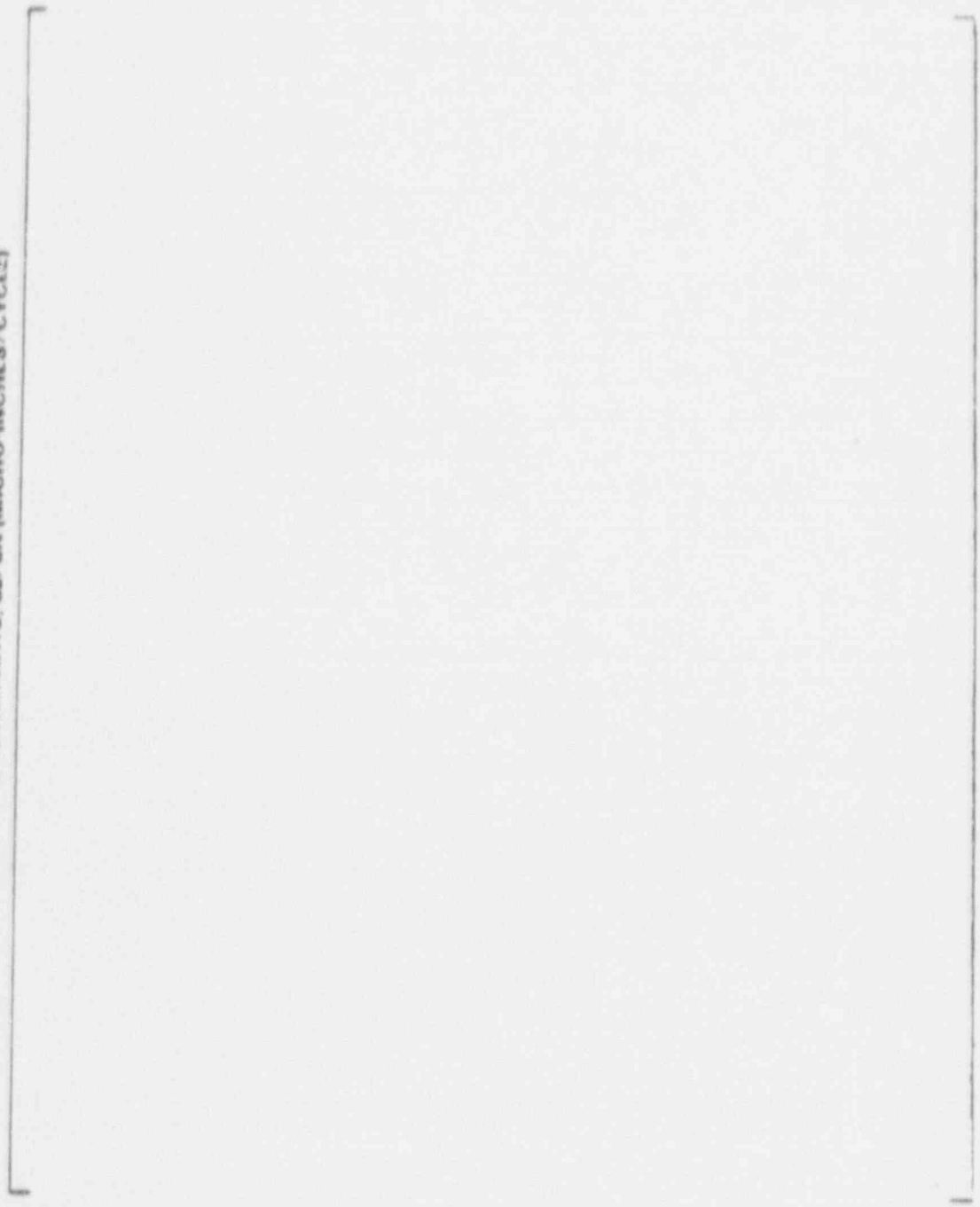

Figure 8-2

Reference Fatigue Crack Growth Curves for [
]a,c,e

[ ]a,c,e

Figure 8-3

Reference Fatigue Crack Growth Law for [ ]a,c,e
in a Water Environment at 600°F

SECTION 9.0
ASSESSMENT OF MARGINS

The results of the leak rates of section 6.4 and the corresponding stability and fracture toughness evaluations of sections 7.1, 7.2 and 7.3 are used in performing the assessment of margins. Margins are shown in Table 9-1.

In summary, at all the critical locations relative to:

1. Flaw Size - Using faulted loads obtained by the absolute sum method, a margin of 2 or more exists between the critical flaw and the flaw having a leak rate of 10 gpm (the leakage flaw).

2. Leak Rate - A margin of 10 exists between the calculated leak rate from the leakage flaw and the leak detection capability of 1 gpm.

3. Loads - At the critical locations the leakage flaw was shown to be stable using the faulted loads obtained by the absolute sum method (i.e., a flaw twice the leakage flaw size is shown to be stable; hence the leakage size flaw is stable).

TABLE 9-1
SUMMARY TABLE

Location	Leakage Flaw Size	Critical Flaw Size	Margin
	[		] a,c,e
1			
3			
12			
	]		]

---

a based on limit load

b based on J integral evaluation

SECTION 10.0
CONCLUSIONS

This report justifies the elimination of RCS primary loop pipe breaks for the Virgil C. Summer nuclear plant as follows:

a. Stress corrosion cracking is precluded by use of fracture resistant materials in the piping system and controls on reactor coolant chemistry, temperature, pressure, and flow during normal operation.

b. Water hammer should not occur in the RCS piping because of system design, testing, and operational considerations.

c. The effects of low and high cycle fatigue on the integrity of the primary piping are negligible.

d. Adequate margin exists between the leak rate of small stable flaws and the capability of the Virgil C. Summer reactor coolant system pressure boundary Leakage Detection System.

e. Ample margin exists between the small stable flaw sizes of item d and larger stable flaws.

f. Ample margin exists in the material properties used to demonstrate end-of-service life (relative to aging) stability of the critical flaws.

For the critical locations flaws are identified that will be stable because of the ample margins in d, e, and f above.

Based on the above, it is concluded that dynamic effects of RCS primary loop pipe breaks need not be considered in the structural design basis of the Virgil C. Summer plant.

APPENDIX A

LIMIT MOMENT

[

]a,c,e

Figure A-1

Pipe with a Through-Wall Crack in Bending

APPENDIX B

TOUGHNESS CRITERIA FOR THE
VIRGIL C. SUMMER CAST PRIMARY LOOP COMPONENTS

All of the individual cast piping components of the Virgil C. Summer primary loop piping satisfy the original [ ]^{a,c,e} criteria (reference 4-5). [

]^{a,c,e}

TABLE B-1

CHEMISTRY AND FRACTURE TOUGHNESS PROPERTIES OF THE
MATERIAL HEATS OF VIRGIL C. SUMMER

a,c,e

[ ] a,c,e

[ ] a,c,e